Multi-User Small-Scale Spectrum Aggregation

Paweł Kryszkiewicz, Adrian Kliks and Hanna Bogucka
Faculty of Electronics and Telecommunication
Poznan University of Technology
Poznan, Poland
Email: pawel.kryszkiewicz — adrian.kliks — hanna.bogucka@put.poznan.pl

***Abstract*—In this paper, we deal with the small-scale spectrum aggregation, where a set of even very narrow and disjoint frequency bands closely located on the frequency axis can be utilized simultaneously. Contrarily to our previous work on that subject, we concentrate on the multiuser scenario in which the 5G system tries to share the spectrum interleaved by multiple narrowband signals realized in the protected cellular systems, e.g., 2G/3G systems. We first present the idea of multiuser small scale sharing based on non-contiguous multicarrier (NC-MC) techniques. In our optimization problem we rely on the detailed interference model that takes into account limitations of both transmitter and receiver frequency selectivity, and which has been practically validated. Presented results confirm that proposed solution can provide high throughput even when the 5G system operates in a dense heterogeneous network.**

I. Introduction

The foresaw need for effective management of continuously increasing mobile traffic [1] has been reflected in the definitions of the so-called Key Performance Indicators (KPIs) which shape the requirements for the next generation wireless systems [2]. It has been recognized that advanced spectrum sharing and aggregation can be the enablers for such 5G networks [3]. For example, mobile network operators (MNOs) can migrate from one (older) technology (e.g., GSM or UMTS) to another one (such as LTE-A, or to a future 5G technology), while keeping both system active and utilizing (refarming) the same frequency bands originally assigned to older technology. Let us highlight the characteristic relation existing between bandwidths of the legacy and new wireless systems: GSM transmission can be treated as *narrowband*, whereas LTE-A and 5G systems can operate on much broader frequency bands (up to 100 MHz). Thus, should the GSM or UMTS users be active, it can happen that the potentially wide vacant spectrum will be split into a number of unused but narrower spectrum resources. Such an observation leads us to the concept of small-scale spectrum aggregation and sharing scheme, which we have initially presented in [4], and where the idea of application of non-contiguous multicarrier systems (NC-MC) for such purpose has been discussed.

In the considered context of spectrum aggregation and systems coexistence, the problem of generated interference among the systems has to be analyzed twofold. First, backward compatibility has to be guaranteed, i.e., the Protected Systems (PSs) should not be distorted by the introduced NC-MC transmission. Here, one needs to consider technical imperfections of the devices: selectivity of the reception filters and non-ideal spectrum emission masks. Second, newer 5G devices will observe a certain level of interference originating from the legacy systems.

In this paper, which is the continuation and significant extension of our previous work [5], we focus on flexible and efficient spectrum aggregation of licensed spectrum in multiuser scenario. In [5] we concentrated on practical validation of the newly proposed interference model, limiting our discussions to the case, where only one narrowband link has to be protected by the 5G system. As the proposed model was successfully validated, we decided to verify the applicability of the small-scale spectrum aggregation scheme in a more practical, multi-user scenario.

In Sec. II, we briefly revisit the concept of small-scale spectrum aggregation in the context of multiuser scenario. Moreover, based on the cross-interference model from [5] we discuss the coexistence framework of 5G NC-MC transmission with a legacy system. Within this framework, we define and solve the NC-MC system-rate optimization problem in Sections III. Numerical results are provided in Section IV. The paper is concluded in Sec. V.

II. Revisiting the Non-Contiguous Multicarrier Schemes as the Small-Scale Spectrum Aggregation Mechanism

Let us now briefly summarize the key ideas of application of NC-MC schemes (such as NC orthogonal frequency division multiplexing, NC-OFDM, or filterbank based multicarrier, NC-FBMC) as an efficient tool for smalls-scale spectrum sharing and aggregation [4], [5].

A. Small-scale spectrum aggregation concept

In a broader sense, spectrum aggregation refers to making use of discontinuous frequency bands. A specific instantiation of this concept tailored to the 4G networks is the so-called carrier aggregation scheme. As a complement to this, small-scale spectrum aggregation can be considered, where instead of so-called component carriers (CCs) known in LTE, the frequency segments of arbitrary (possibly narrow) bandwidths can be assigned to particular users or systems. For example, an operator may share own-licensed spectrum among various technologies (e.g., GSM and 5G, LTE Release 8 and 5G, etc.).

B. Non-contiguous multicarrier schemes

We assume that at the NC-MC transmitter (TX) the data-bits are mapped to QAM/PSK complex symbols and fed to

N_d inputs of N-size IFFT ($N_\mathrm{d} \leq N$). The set of N_d occupied subcarriers indices $\mathbf{I}_\mathrm{DC} \subset \left\{-\frac{N}{2}, \ldots, \frac{N}{2}-1\right\}$ is controlled by a dedicated steering block. This block is a main modification needed for NC-MC transmission in comparison to contiguous-MC transmission. The complex symbol (zero or QAM/PSK) modulating the n-th subcarrier ($n \in \left\{-\frac{N}{2}, \ldots, \frac{N}{2}-1\right\}$) in the m-th MC symbol is denoted as $d_{n,m}$. After IFFT and whole baseband (BB) processing the time-domain samples s_k are created. Assuming that the signal is sampled with frequency $f_s = N\Delta f$, where Δf defines the subcarrier spacing, the discrete NC-MC signal can be described as:

$$s_k = \sum_{m\in\mathbb{Z}} \sum_{n=-\frac{N}{2}}^{\frac{N}{2}-1} d_{n,m} \overbrace{\phi\left[k-mM\right] e^{\left(\imath \frac{2\pi n}{N}(k-mM)\right)}}^{\phi_{n,m}[k]} \quad (1)$$

where $\phi_{n,m}[k]$ is the original pulse shape $\phi[k]$ shifted in time and in frequency by mM samples and n subcarriers respectively, $\mathbb{Z}$ is the set of integers, and $\imath^2 = -1$. In general, M and Δf can be understood as the time and frequency distance between two consecutive and adjacent pulses on the time-frequency plane. If we limit the time-span to one multicarrier symbol, so that index m in $d_{n,m}$ is omitted, the NC-MC symbol frequency representation $S(\omega)$ at normalized pulsation $\omega \in \langle -\pi, \pi \rangle$ can be obtained by Fourier transformation of a time domain signal s_k as in [6], [7]: $S(\omega) = \sum_{n=-\frac{N}{2}}^{\frac{N}{2}-1} d_n S^\mathrm{TX}(\omega, n)$, where $S^\mathrm{TX}(\omega, n)$ is the n-th subcarrier frequency response. At the NC-MC receiver, the dual pulse-shaping filtering is applied. In the case of signal perfect-reconstruction, the RX filter characteristic is a complex conjugate of the TX filter, thus, $|S^\mathrm{RX}(\omega, n)| = |S^\mathrm{TX}(\omega, n)|$. The exemplifications of the above observations to NC-OFDM and NC-FBMC have been presented in details in [5].

C. Interference analysis

Let us consider a generic downlink case[1], where the future 5G wireless system will be deployed in the same area as other, already existing PSs that have to be protected from harmful interference. Such a situation is illustrated in Fig. 1, where in its part A one can observe two systems - two PSs and the new (spectrally-flexible) 5G one. The user equipment j to be protected (PS $\mathrm{UE}_{i,j}$) receives the signal from its system BS_i (with power attenuation $\alpha_{\mathrm{PS}_i-\mathrm{PS}_{i,j}}$ and frequency frequency response $H_{\mathrm{PS}_i-\mathrm{PS}_{i,j}}(f)$), and observes interference from the coexisting system (via the channel of power attenuation $\alpha_{5\mathrm{G}-\mathrm{PS}_i}$ and frequency response $H_{5\mathrm{G}-\mathrm{PS}_i}(f)$). Similarly, the 5G UE detects not only the wanted NC-MC signal from its BS (via the channel of power-attenuation $\alpha_{5\mathrm{G}-5\mathrm{G}}$ and frequency response $H_{5\mathrm{G}-5\mathrm{G}}(f)$), but also interfering signal from incumbent PS (passing the channel of power-attenuation $\alpha_{\mathrm{PS}_i-5\mathrm{G}}$ and frequency response $H_{\mathrm{PS}_i-5\mathrm{G}}(f)$). In Fig. 1a, the wanted signal is denoted by solid line, whereas interference - by dotted line. Our considerations focus on maximization of the rate achieved in the 5G system while fully protecting the incumbent users, taking limitations caused by the non-ideal nature of the transmit and reception filters into account. Interference to PS1 or PS2 results from the unwanted emission of the coexisting NC-MC TX out of the nominal band (known as out-of-band-emission - OOBE, typically limited by the definition of so-called spectrum-emission-masks (SEM) or adjacent channel leakage ratio (ACLR)). Moreover, non-ideal RX filters with limited selectivity (described by the adjacent channel selectivity metric, ACS) gather the signal frequency components not only from the wanted frequency band, but also outside of it. These two cases are presented graphically as parts *B* and *C* in Fig. 1.

[1] Analogous derivations can be repeated for the uplink case.

If the power-attenuation of any considered downlink channel (including pathloss and antennas gains) is denoted by α, and the channel frequency response by $H_{\mathrm{TX-RX}}(f)$, the received interference power can be expressed as:

$$P_\mathrm{I} = \alpha \int_{-\infty}^{\infty} \Upsilon^\mathrm{TX}(f-f_c) \left|H^\mathrm{RX}(f-f_c)\right|^2 \left|H_\mathrm{TX-RX}(f-f_c)\right|^2 df, \quad (2)$$

where f_c is the center frequency of a considered system, $\Upsilon^\mathrm{TX}(f)$ is the power spectral density at the TX output (either PS or 5G base station) at frequency f and $H^\mathrm{RX}(f)$ is a frequency response of an RX filter (either PS or 5G terminal). This interference model, used hereafter, was validated in [5].

III. Multiuser Small-Scale Spectrum Aggregation - Problem Formulation

We look at the system rate maximization for 5G system by adjusting the power transmitted by 5G BS on each subcarrier P_n ($n \in \mathbf{I}_\mathrm{DC}$) subject to identified constraints. In the considered scenario we want to protect more links than one. From the spectrum utilization point of view, more active links corresponds to more *gaps* in the considered frequency band (more fragmented spectrum), which have to be protected. Let us denote the number of active links (systems) in a certain geographical vicinity as B, what means that there will be B interference constrains. We concentrate on capacity maximization assuming only the pathloss known (fading unknown), as it was shown to be an effective approach for long term power allocation [5]. $\alpha_{\mathrm{PS}_b-5\mathrm{G}}$ stands for the channel attenuation between the b-th PS BS and 5G UE.

The goal is to maximize the Shannon data rate:

$$\mathbf{P}^* = \arg\max_{\mathbf{P}} \quad (3)$$
$$\Delta f \chi \sum_{n\in\mathbf{I}_\mathrm{DC}} \log_2\left(1 + \frac{\alpha_{5\mathrm{G}-5\mathrm{G}} P_n}{F N_0 \Delta f + \sum_{b=1}^{B} \alpha_{\mathrm{PS}_b-5\mathrm{G}} P_{\mathrm{I}n,b}^\mathrm{RX}}\right)$$

where N_0 is a white noise power spectral density, and F is noise figure of 5G receiver, $P_{\mathrm{I}n,b}^\mathrm{RX}$ stands for the interference observed at the nth subcarrier and originated from the bth PS transmitter. Moreover, χ is the rate-scaling factor accounting for the symbol duration extension (e.g. application of cyclic prefix, CP). It is equal to 1 in the ideal case (when no CP is used) or FBMC, and equal to $N/(N + N_\mathrm{CP})$ in case of an OFDM or NC-OFDM system, which typically uses CP. In our optimization problem we consider the following requirements.

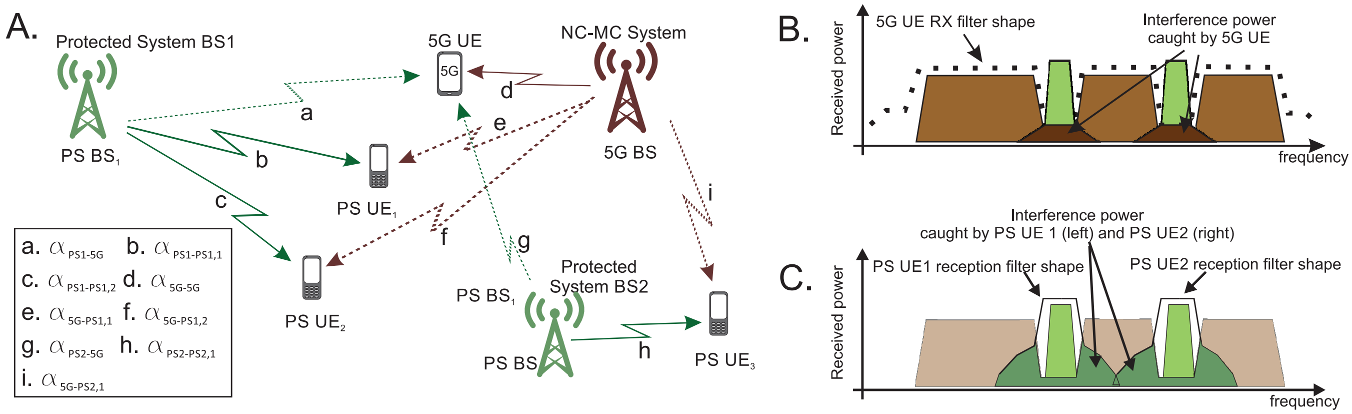

Fig. 1. Illustration of the coexistence of two wireless systems: two existing PS and the spectrally-flexible (applying NC-MC scheme) 5G system.

QoS requirements: The 5G system should guarantee the QoS required by PS system. If $\mathrm{SIR}_{\min,b}$ is the minimum signal-to-interference ratio (SIR) required by the bth PS, than

$$\frac{P_{\mathrm{RX}}^{\mathrm{PS}_b\ \mathrm{UE}}}{\sum_{n\in\mathbf{I}_{\mathrm{DC}}}\alpha_{5\mathrm{G}-\mathrm{PS}_b}P_n g_n}\geq \mathrm{SIR}_{\min}, \quad (4)$$

where g_n can be interpreted as the coupling factor between the power transmitted on the n-th subcarrier observed at victim receivers antenna and the effective interference power degrading victims reception (see [5] for details). $P_{\mathrm{RX}}^{\mathrm{PS}_b\ \mathrm{UE}}$ is useful signal power received by PS RX defined as

$$P_{\mathrm{RX}}^{\mathrm{PS}_b\ \mathrm{UE}}=\alpha_{PS_b-PS_b}\int_{-\pi}^{\pi}\Upsilon_{\mathrm{PS},b}^{\mathrm{TX}}\left(\frac{\omega f_s}{2\pi}\right)d\omega, \quad (5)$$

$\Upsilon_{\mathrm{PS},b}^{\mathrm{TX}}\left(\frac{\omega f_s}{2\pi}\right)$ is PSD of the bth PS at its transmitter.

Requirements on the transmit power: Next, a maximum power of the 5G transmitter should be limited giving

$$\sum_{n\in\mathbf{I}_{\mathrm{DC}}}P_n\leq P_{\mathrm{MAX}}, \quad (6)$$

where P_{MAX} is a maximum allowed power of 5G transmitter. The last constraints guarantee that power on each subcarrier is equal or greater than 0, i.e.,

$$\forall_{n\in\mathbf{I}_{\mathrm{DC}}}P_n\geq 0. \quad (7)$$

As the inequality constrained nonlinear optimization problem is defined, one may introduce the Karush-Kuhn-Tucker multipliers μ_n, β_b and λ and apply them for a definition of a corresponding Lagrangian function $J(P_n,\lambda,\beta_b,\mu_n)$. Then, the KKT necessary conditions used to solve this problem are:

$$\forall_{n\in\mathbf{I}_{\mathrm{DC}}}\frac{\partial J(P_n,\lambda,\beta_b,\mu_n)}{\partial P_n}=0, \quad (8)$$

$$\forall_{b\in\{1,2,\ldots,B\}}\beta_b\left(\sum_{n\in\mathbf{I}_{\mathrm{DC}}}\alpha_{5\mathrm{G}-\mathrm{PS}_b}P_n g_{n,b}-\frac{P_{\mathrm{RX}}^{\mathrm{PS}_b\ \mathrm{UE}}}{\mathrm{SIR}_{\min}}\right)=0, \quad (9)$$

$$\lambda\left(\sum_{n\in\mathbf{I}_{\mathrm{DC}}}P_n-P_{\mathrm{MAX}}\right)=0, \quad (10)$$

$$\forall_{n\in\mathbf{I}_{\mathrm{DC}}}\mu_n\left(-P_n\right)=0, \quad (11)$$

where $\forall_{n\in\mathbf{I}_{\mathrm{DC}}}\mu_n\geq 0$, $\beta_b\geq 0$ and $\lambda\geq 0$. The result of (8) is

$$P_n=\frac{\Delta f\chi}{\ln(2)\left(\lambda+\sum_{b=1}^{B}\beta_b\alpha_{5\mathrm{G}-\mathrm{PS}_b}g_{n,b}-\mu_n\right)}-Q_n, \quad (12)$$

where

$$Q_n=\frac{FN_0\Delta f+\sum_{b=1}^{B}\alpha_{\mathrm{PS}_b-5\mathrm{G}}P_{\mathrm{In},b}^{\mathrm{RX}}}{\alpha_{5\mathrm{G}-5\mathrm{G}}} \quad (13)$$

that should be substituted to formulas (9)-(11) in order to find the multipliers values. For each constraint two possibilities have to be considered: the multiplier equals zero and the constraint is inactive or the multiplier is positive and the constraint is active. In the case of (11), when this constraint is active for the n-th subcarrier, the power of n-th subcarrier has to be set to zero. In general, every combination of N_d+1+B multipliers being active or inactive should be considered, i.e., 2^{N_d+1+B} cases. However, an algorithm presented below allows to decrease the number of combinations to be considered, e.g., when (9) is active and on some subcarriers $P_n<0$, respective equations (11) have to be *activated*, which increases interference to the PS, so that (9) has to be still active. Let us first derive solutions for some special cases. It is assumed that $\mathbf{I}_{\mathrm{cons}}\subset\mathbf{I}_{\mathrm{DC}}$ of size γ is a set of indices n for which μ_n is positive, i.e., $P_n=0$. Let us consider the following cases:

- If $\forall_{b\in\{1,2,\ldots,B\}}\beta_b=0$ and $\lambda\neq 0$, i.e., 5G BS is limited by available power, the interference induced to all PS UEs is below the limit, substitution of (12) and $\mu_n=0$ for $n\in\mathbf{I}_{\mathrm{DC}}\backslash\mathbf{I}_{\mathrm{cons}}$ and $P_n=0$ for $n\in\mathbf{I}_{\mathrm{cons}}$ into (10) gives

$$\lambda=\frac{\Delta f\chi(N_d-\gamma)/\ln(2)}{\sum_{n\in\mathbf{I}_{\mathrm{DC}}\backslash\mathbf{I}_{\mathrm{cons}}}Q_n+P_{\mathrm{MAX}}}, \quad (14)$$

- If $\lambda=0$, $\beta_b\neq 0$ and $\forall_{i\in\{1,2,b-1,b+1,\ldots,B\}}\beta_i=0$, i.e., only the interference to the bth PS is constrained giving:

$$\beta_b=\frac{\Delta f\chi(N_d-\gamma)/\ln(2)}{\sum_{n\in\mathbf{I}_{\mathrm{DC}}\backslash\mathbf{I}_{\mathrm{cons}}}\alpha_{5\mathrm{G}-\mathrm{PS}_b}g_{n,b}Q_n+\frac{P_{\mathrm{RX}}^{\mathrm{PS}_b\ \mathrm{UE}}}{\mathrm{SIR}_{\min}}}, \quad (15)$$

- If there is more than one multiplier active out of set $\{\lambda,\beta_1,\ldots,\beta_B\}$, a set of nonlinear equations obtained after substitution of (12) and $\mu_n = 0$ for $n \in \mathbf{I}_{\mathrm{DC}} \setminus \mathbf{I}_{\mathrm{cons}}$ and $P_n = 0$ for $n \in \mathbf{I}_{\mathrm{cons}}$ into (9) and (10) has to be solved:

$$\forall_{b\in\{1,2,\ldots,B\}} f1_b(\beta_1,\beta_2,\ldots,\beta_B,\lambda) = \alpha_{5\mathrm{G-PS}_b} \cdot \sum_{n\in\mathbf{I}_{\mathrm{DC}}\setminus\mathbf{I}_{\mathrm{cons}}} g_{n,b}\left(\frac{\Delta f\chi/\ln(2)}{\lambda+\sum_{q=1}^{B}\alpha_{5\mathrm{G-PS}_q} g_{n,q}} - Q_n\right) - \frac{P_{\mathrm{RX}}^{\mathrm{PS}_b\ \mathrm{UE}}}{\mathrm{SIR}_{\mathrm{min,b}}} = 0, \tag{16}$$

$$f2(\beta_1,\beta_2,\ldots,\beta_B,\lambda) = \sum_{n\in\mathbf{I}_{\mathrm{DC}}\setminus\mathbf{I}_{\mathrm{cons}}}\left(\frac{\Delta f\chi}{\ln(2)\left(\lambda+\sum_{b=1}^{B}\alpha_{5\mathrm{G-PS}_b} g_{n,b}\right)} - Q_n\right) - P_{\mathrm{MAX}} = 0. \tag{17}$$

As the Newton method is applied, the derivatives for application of that algorithm can be calculated as follows:

$$\forall_{b\in\{1,2,\ldots,B\}} \frac{\partial f1_b(\beta_1,\beta_2,\ldots,\beta_B,\lambda)}{\partial\lambda} = \sum_{n\in\mathbf{I}_{\mathrm{DC}}\setminus\mathbf{I}_{\mathrm{cons}}} -\frac{\Delta f\chi}{\ln(2)} \frac{\alpha_{5\mathrm{G-PS}_b} g_{n,b}}{\left(\lambda+\sum_{q=1}^{B}\alpha_{5\mathrm{G-PS}_q} g_{n,q}\right)^2} \tag{18}$$

$$\forall_{b\in\{1,2,\ldots,B\}}\forall_{v\in\{1,2,\ldots,B\}} \frac{\partial f1_b(\beta_1,\beta_2,\ldots,\beta_B,\lambda)}{\partial\beta_v} = \sum_{n\in\mathbf{I}_{\mathrm{DC}}\setminus\mathbf{I}_{\mathrm{cons}}} -\frac{\Delta f\chi}{\ln(2)} \frac{\alpha_{5\mathrm{G-PS}_b} g_{n,b}\cdot\alpha_{5\mathrm{G-PS}_v} g_{n,v}}{\left(\lambda+\sum_{q=1}^{B}\alpha_{5\mathrm{G-PS}_q} g_{n,q}\right)^2} = \tag{19}$$

$$\frac{\partial f1_v(\beta_1,\beta_2,\ldots,\beta_B,\lambda)}{\partial\beta_b} \tag{20}$$

$$\frac{\partial f2(\beta_1,\beta_2,\ldots,\beta_B,\lambda)}{\partial\lambda} = \sum_{n\in\mathbf{I}_{\mathrm{DC}}\setminus\mathbf{I}_{\mathrm{cons}}} -\frac{\Delta f\chi}{\ln(2)} \frac{1}{\left(\lambda+\sum_{q=1}^{B}\alpha_{5\mathrm{G-PS}_q} g_{n,q}\right)^2} \tag{21}$$

$$\forall_{v\in\{1,2,\ldots,B\}} \frac{\partial f2(\beta_1,\beta_2,\ldots,\beta_B,\lambda)}{\partial\beta_v} = \frac{\partial f1_b(\beta_1,\beta_2,\ldots,\beta_B,\lambda)}{\partial\lambda}. \tag{22}$$

The $k-th$ iterative improvement of values λ and $\forall_{b\in\{1,2,\ldots,B\}}\ \beta_b$ can be described as:

$$\begin{bmatrix}\lambda_{k+1}\\ \beta_{1,k+1}\\ \cdots\\ \beta_{B,k+1}\end{bmatrix} = \begin{bmatrix}\lambda_{k}\\ \beta_{1,k}\\ \cdots\\ \beta_{B,k}\end{bmatrix} - \epsilon\begin{bmatrix}\Delta\lambda_{k}\\ \Delta\beta_{1,k}\\ \cdots\\ \Delta\beta_{B,k}\end{bmatrix}, \tag{23}$$

where $\epsilon \in \langle 0;1\rangle$ is update scaling factor, and the entries in the last matrix are defined as in (24) at the top of next page, where we use the simplified notation $\mathbf{B} = [\beta_1,\beta_2,\ldots,\beta_B]$. While Newton method guarantees fast convergence, it is important to guarantee that multipliers β_b and λ lie within their feasible region, i.e. $\lambda \geq 0$ and $\beta_b \geq 0$. It is done by adjustment of ϵ parameter, so that

$$\epsilon_{\beta b} = \begin{cases}\frac{\beta_b}{\Delta\beta_b} & \text{for} \quad \Delta\beta_b > 0\\ 1 & \text{for} \quad \Delta\beta_b \leq 0\end{cases}, \tag{25}$$

$$\epsilon_{\lambda} = \begin{cases}\frac{\lambda_k}{\Delta\lambda_k} & \text{for} \quad \Delta\lambda_k > 0\\ 1 & for \quad \Delta\lambda_k \leq 0\end{cases}, \tag{26}$$

and

$$\epsilon = 0.98\min\{1,\epsilon_{\beta 1},\ldots,\epsilon_{\beta B},\epsilon_{\lambda}\}, \tag{27}$$

where value 0.98 was chosen to guarantee strict feasibility of the solution. The set of the constrained subcarriers $\mathbf{I}_{\mathrm{cons}}$ is updated in each iteration. Empirically, λ and β_b obtained in the previous iteration can be used in the next one providing fast Newton method convergence. Block diagram of the solution is presented in Fig. 2. If at least two multipliers out of set $\{\lambda,\beta_1,\ldots,\beta_B\}$ have to be activated, it is done iteratively, starting with all combinations of 2 multipliers. If it does not succeed, all combinations of 3 multipliers active are tested etc.

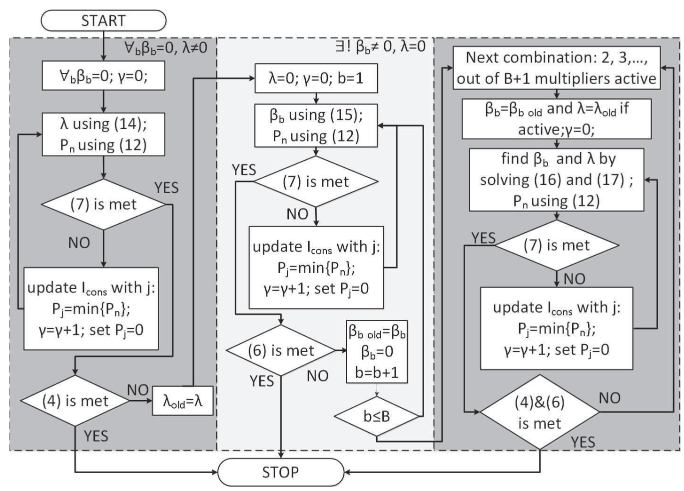

Fig. 2. Block scheme for the solution of optimization problem.

IV. Simulation results

In order to evaluate the correctness of the proposed solution we have carried out intensive computer simulations, where we maximized the throughput of the 5G system in the scenario presented in Fig. 3. Beside the 5G network operating at frequency 1850 MHz, one may observe the presence of PS, i.e., the fragment of GSM network consisting of two base stations with transmit power equal to 40 and 37 dBm, located 3 km away from each other, and operating frequencies $f_1 = 1849.6$ MHz and $f_2 = 1850.6$ MHz. Each GSM base station serves many users, but only the specific subset of them is shown in that figure, i.e., the users that are mostly affected by the 5G base station. The transmit power of the 5G base station is intentionally set to high value, i.e, 37 dBm. The colors applied to base stations and UEs show, which UE is connected to which base station. There is also a red

$$
\begin{bmatrix} \Delta\lambda_k \\ \Delta\beta_{1,k} \\ \dots \\ \Delta\beta_{B,k} \end{bmatrix} = \begin{bmatrix} \frac{\partial f2(\mathbf{B},\lambda)}{\partial \lambda} & \frac{\partial f2(\mathbf{B},\lambda)}{\partial \beta_1} & \dots & \frac{\partial f2(\mathbf{B},\lambda)}{\partial \beta_B} \\ \frac{\partial f1_1(\mathbf{B},\lambda)}{\partial \lambda} & \frac{\partial f1_1(\mathbf{B},\lambda)}{\partial \beta_1} & \dots & \frac{\partial f1_1(\mathbf{B},\lambda)}{\partial \beta_B} \\ \dots & \dots & \dots & \dots \\ \frac{\partial f1_B(\mathbf{B},\lambda)}{\partial \lambda} & \frac{\partial f1_B(\mathbf{B},\lambda)}{\partial \beta_1} & \dots & \frac{\partial f1_B(\mathbf{B},\lambda)}{\partial \beta_B} \end{bmatrix}^{-1} \Bigg|_{\beta_{1,k},\beta_{2,k},\dots,\beta_{B,k},\lambda_k} \begin{bmatrix} f2(\beta_{1,k},\beta_{2,k},\dots,\beta_{B,k},\lambda_k) \\ f1_1(\beta_{1,k},\beta_{2,k},\dots,\beta_{B,k},\lambda_k) \\ \dots \\ f1_B(\beta_{1,k},\beta_{2,k},\dots,\beta_{B,k},\lambda_k) \end{bmatrix}, \quad (24)
$$

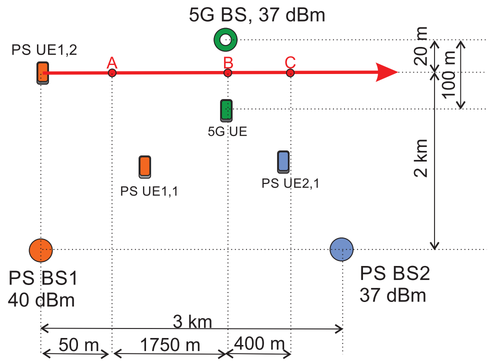

Fig. 3. Simulation scenario - identification of the route of the protected PS UE1,2.

route shown in Fig. 3, which shows how the GSM mobile user is moving from one cell to another, i.e., we assume that the handover procedure starts when received power from PS BS2 is higher than the power received from PS BS1. The three points, A-C, represents three specific cases - in position A the PS UE1,2 is served by the first GSM base station (orange) at arbitrarily selected frequency f_1 and is relatively far away from the 5G transmitter. In position B, the GSM mobile user is very close to the high power 5G base station, thus it may observe high interference coming from the 5G system. In point C, second base station serves the mobile user at the new frequency channel, which center frequency is f_2. The pathloss is calculated using the Log-distance model with pathloss exponent equal to 3. Antenna gains equal 15 dBi and 0 dBi at BS and UE, respectively. All of the simulations have been carried assuming known AWGN power equal to thermal noise (-174 dBm/Hz) increased by 12 dB noise figure. The following simulation parameters have been used: $\mathrm{SIR}_{\mathrm{min}} = 9$ dB, IFFT size was equal to 256, and the subcarriers indexed $\{-90, ..., -1\} \cup \{1, ..., 90\}$ were available for 5G system for power allocation. Subcarrier spacing equals $\delta f = 15$ kHz. Moreover, as in [5] we verified a few types of NC-MC systems, i.e., the NC-OFDM with the cyclic prefix of 16 samples, NC-OFDM with windowing (each symbol extended by 16 window samples), and NC-FMBC with the K factor of the PHYDYAS filter set to 2 and 4. Additionally, *perfect* case with rectangular TX/RX filter is considered. In Fig. 4 one may observe the mean throughput as the function of the PS UE1,2 location. The achieved throughput is low only in a worst case, i.e., when the GSM mobile user that has to be protected is very close to 5G BS (around 2000 m from the beginning of the route). In all other cases the adaptive algorithm proposed in this paper efficiently allocates the power across the available subcarriers protecting GSM users, maximizing the rate of the 5G system. It is worth mentioning that the best results have been obtained for the perfect filters and NC-FBMC scheme with K=4, as this guarantees high frequency selectivity of the applied filters. However, all the NC-MC schemes outperform significantly standard OFDM in terms of throughput when PS UE is nearby.

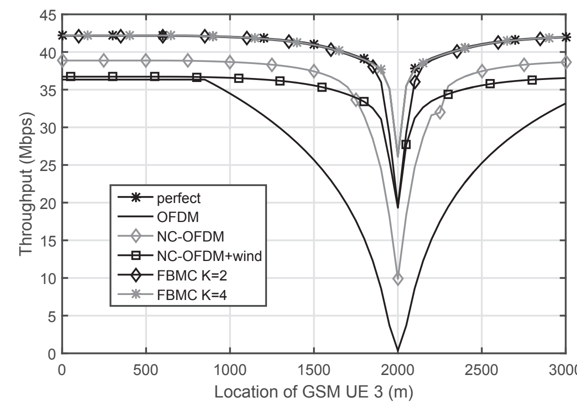

Fig. 4. Mean throughput observed by the 5G user as the function of the position of the PS UE1,2.

In the next three figures we show, how the power has been allocated among the subcarriers by 5G BS in three identified points: A (Fig. 5), B (Fig. 6) and C (Fig. 7). One may observe that in first position the proposed algorithm protects the PS UE1,2 and PS UE2,1 by reducing the power allocated in these subcarriers whose overlap the GSM signal channels (around frequencies f_1 and f_2). As the users of the orange base stations are more far away from the 5G BS more power can be assigned to the subcarriers that overlap GSM channel f_1. When the GSM mobile user arrives in location B, strong protection gap around the frequency f_1 needs to be created resulting in overall reduction of the rate in 5G network. In that point the GSM mobile user is still served by orange base station. In point C, however, one may notice that the gap with inactive subcarriers (no power has been assigned to these subcarriers) around GSM channel f_2 is large, as the GSM mobile users is now served by the blue GSM base station. Observe that in points B and C power allocated on subcarriers is negligible in comparison to the other schemes. Additionally, it can be observed that high selectivity of TX/RX filters, e.g., in the perfect case or while using FBMC scheme, allows for steeper power allocation scheme and narrower notch around PS carrier.

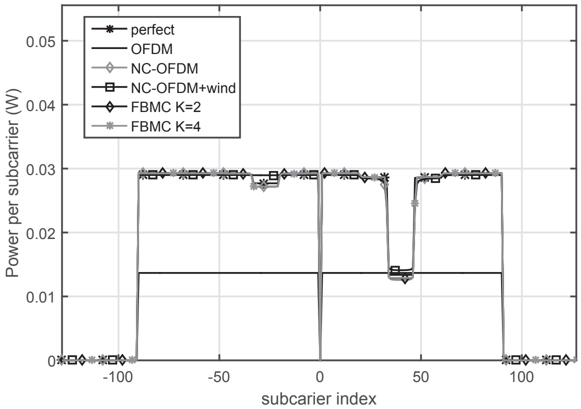

Fig. 5. Power allocated among subcarriers in 5G system while the GSM mobile user is located at point A.

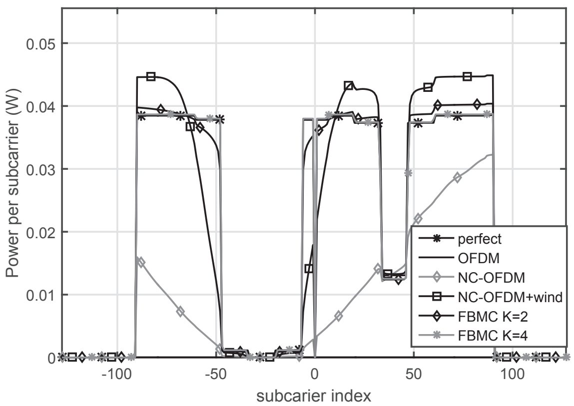

Fig. 6. Power allocated among subcarriers in 5G system while the GSM mobile user is located at point B.

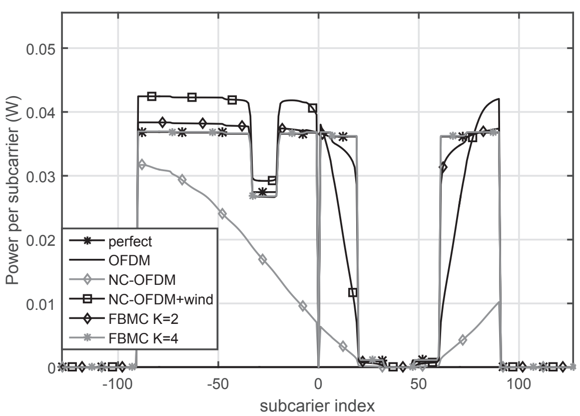

Fig. 7. Power allocated among subcarriers in 5G system while the GSM mobile user is located at point C.

V. Discussion and Conclusions

In this work we have examined the feasibility of the low-scale spectrum aggregation concept in a multiuser scenario. We claimed that such a non-contiguous nature of the utilized spectrum entails the natural selection of various multicarrier transmission schemes, which are considered as the main candidates for 5G systems anyway. In our work we have arbitrarily selected one type of signals that have to be protected - a GSM network with multiple users. This selection was made to illustrate the possibility of smooth transition of frequency assignment from older to newer technologies while keeping the electromagnetic compatibility with origin systems. The achieved results shown that the 5G network can achieve reasonable throughput while protecting the coexisting legacy systems. However, in order to apply the proposed algorithm, both transmit and reception filter characteristics (or their estimates) have to be known to the 5G user, second, the channel information (at least about the attenuation) has to be distributed in the system. As the latter is often required for other purposes anyway (such as for advanced radio-resource or interference management techniques), the main problem remains with the evaluation of the filter shapes. Fortunately, one can apply the worst case scenario, i.e. for the transmit filters one can use the definition of spectrum emission masks that can be found in the standards. The reception filter characteristic, however, should be somehow measured or assessed based on some past experiments, as we did in our work.

Acknowledgment

The work has been funded by the EU H2020 project COHERENT (contract no. 671639).

References

[1] Cisco, “Cisco Visual Networking Index: Global mobile data traffic forecast update, 20152020,” Tech. Rep., February 2016. [Online]. Available: http://www.cisco.com/c/en/us/solutions/collateral/service-provider/visual-networking-index-vni/mobile-white-paper-c11-520862.pdf

[2] 5GPPP, “Cisco Visual Networking Index: Global mobile data traffic forecast update, 20152020,” Tech. Rep., April 4th (date accessed) 2016. [Online]. Available: https://5g-ppp.eu/kpis/

[3] M. Mustonen, M. Matinmikko, M. Palola, S. Yrjl, and K. Horneman, “An evolution toward cognitive cellular systems: licensed shared access for network optimization,” *IEEE Communications Magazine*, vol. 53, no. 5, pp. 68–74, May 2015.

[4] H. Bogucka, P. Kryszkiewicz, and A. Kliks, “Dynamic spectrum aggregation for future 5G communications,” *IEEE Communications Magazine*, vol. 53, no. 5, pp. 35–43, May 2015.

[5] P. Kryszkiewicz, A. Kliks, and H. Bogucka, “Small-scale spectrum aggregation and sharing,” *IEEE Journal on Selected Areas in Communications*, vol. PP, no. 99, pp. 1–1, 2016.

[6] H. Yamaguchi, “Active interference cancellation technique for mb-ofdm cognitive radio,” in *Microwave Conference, 2004. 34th European*, vol. 2, oct. 2004, pp. 1105 –1108.

[7] P. Kryszkiewicz, H. Bogucka, and A. Wyglinski, “Protection of primary users in dynamically varying radio environment: practical solutions and challenges,” *EURASIP Journal on Wireless Communications and Networking*, vol. 2012, no. 1, p. 23, 2012. [Online]. Available: http://jwcn.eurasipjournals.com/content/2012/1/23